POLITECNICO DI TORINO
Repository ISTITUZIONALE

Stability analysis of a parametrically excited ball bearing system

(Article begins on next page)

19 April 2024

Stability analysis of a parametrically excited ball bearing system

Ghasem Ghannad Tehrani, Chiara Gastaldi, Teresa M. Berruti

ARTICLE INFOR

Abstract

In this paper, the stability analysis of a ball bearing system experiencing varying stiffness coefficients is taken into account. The presence of variable stiffness may cause the system to experience instabilities at given combinations of rotational speed, number, and the dimension of balls, thus complicating the design process. The objective is to obtain the stability boundary curves (SBCs) which separate the stable and unstable regions. The well – known Mathieu equation is adopted as the governing equations of the system in horizontal and vertical directions. In order to calculate the SBCs the equations of motion are solved applying approximate methods such as the harmonic balance method (HBM) and the multiple scales method (MSM). This procedure is straightforward if Uncoupled Mathieu equations, either Damped or Undamped, are considered, however, a realistic bearing system can be effectively described only using two coupled Mathieu equations, thus introducing two dominant frequencies which are not an integer coefficient of each other. This last Damped and Coupled set of equations applied to a bearing system is, for the first time, solved using HBM in place of resorting to cost intensive iterative methods. The accuracy of all investigated cases, Uncoupled – Undamped, Uncoupled – Damped and Coupled – Damped, is ensured by Floquet Theory.

1. Introduction

Rolling elements are one of the most important parts of rotating machinery. In the last decades, considerable effort has been put in the modeling of such systems.

A review of the rotor – rolling bearing systems, including FE modeling, is performed by Cao et. al. [1]. Metsebo [2] models a rolling bearing system where the contact is modeled as a varying stiffness in the bearing system. Harsha [3] and Vakharia et. al. [4] make use of the Hertz contact theory to model the bearing stiffness. Bai et. al. [5] perform a stability analysis of a model of rotor – rolling bearing system considering the effect of nonlinearity due to Hertzian contact, De Moerlooze et. al. [6] investigates the influence of rolling element leaning on a flat plate or V – grooved tracks considering the friction in the contact. Guo and Parker [7] computed the time – varying stiffness of a rolling bearing system considering the contact between the rolling elements and the race ways. H Miao et. al. [8] proposed a dynamic similarity design method for a rotor – bearing system and developed a corresponding test rig to determine the dynamic characteristic of a full model structure.

Although rolling elements are mainly applied as a support for the main system to bear axial and vertical loads, they may become an internal generator of instability. One of the causes of these undesirable vibrations is the parametric excitation due to varying stiffness of the rolling bearing during operation. This internal excitation can give rise to many unstable regions where bearings would operate critically. Systems with parametric excitations are typically described using Mathieu Equations. In this instance, however, the "standard" 1D Mathieu Equation has to be substituted with a 2D coupled system of equations to account for the two in-plane Degrees of Freedom (DOFs) of the bearing balls, as described by Srinath et. al. [9].

The goal of this paper is to obtain stability boundary curves across the complete input parameter space. A more efficient method is therefore needed. For this reason, an extensive literary review of the most common cost-effective solution methods of Mathieu equations has been carried out.

Study of Mathieu Equations, both linear and nonlinear, has been performed by Kovacic et. al. [10]. R. Rand dedicated a broad study to nonlinear vibrations including Mathieu Equations [11]. The application of the Perturbation method to investigate the resonance frequencies of non–homogeneous and nonlinear Mathieu Equation has been carried out respectively by Younesian et. al. [12] and Yusry [13]. C. S. Hsu [14] and W. Szemplii [15] dedicated special attention to analyze a multi – degree of freedom coupled system having parametric excitation. The more practical study of parametric excitation in systems such as rotating cylindrical shell and Jeffcott rotor is performed by Han et al. [16] and Hand and Chu [17, 18]. The dynamic analysis of Jeffcott rotor considering the

rotor – stator contact which is another form commonly occurring parametric excitation phenomena is done by Vlajic et al. [19 ,20] and Alzibde et al. [21]. The application of Perturbation methods for solving the nonlinear equation is studied by Nayfeh and Balachndran [16]. Nayfeh and Mook [17] proposed a more advanced application of Perturbations methods for analyzing nonlinear equations. Perturbation methods are only one of the possible solution techniques typically applied to Mathieu Equation. Bakri et. al. [18] performed a stability analysis of a two – degree of freedom nonlinear system applying the Harmonic balance method. A more thorough study of the Harmonic Balance method targeting the non-linear vibration problems is studied by Zucca and Epureanu [19] and Krack and Gross [20].

In this paper approximate methods such as harmonic balance and multiple scales, are applied to provide the roller bearing designer with a complete picture of the stability boundary curves, which are obtained in a timely manner, compatible with the design process.

The present paper is structured as follows: Sect. 2 describes the physical system, while Sect. 3 presents the corresponding set of Mathieu equations describing the system from Sect. 2. Sections 4, 5 and 6 give a brief overview of the methods used throughout the paper. In detail, Sect. 4 addresses the Floquet theory, here used solely as a mean to check the validity of the results obtained through the approximate methods (Multiple Scales and Harmonic Balance) described in Sect. 5 and 6 respectively. Section 7 presents the results obtained on the bearing system in a variety of configurations. The Undamped Uncoupled case is used as a starting point, before addressing the effect of damping and finally that of coupling between the two degrees of freedom.

2. Mathematical Modeling of Bearing System

A ball bearing system comprises of four main components: Balls, Caging, Inner Race and Outer race. These components are all depicted in Figure 1a, except the cage whose interaction with the balls is neglected here. The same bearing can also be represented as a system with springs as shown in Fig. 1b. The balls of the bearing are modeled as springs to highlight the fact that they provide the main contribution to the deformability of the dynamic system. It is important to note that, since the bearing rotates, its total stiffness, by which it supports the shaft, is not constant but varies over time. This can be deduced from the scheme of Figure 2: when the inner ring rotates (here clockwise) under a vertical load F, only the springs in the lower half of the bearing are loaded and the number and position of the loaded springs changes depending on the rotation angle, (see Figure 2 b and Figure 2 c). This variability of the stiffness over time induce in the system a kind of internal excitation, which is called "parametric excitation". Another point which should be mentioned is the existence of the cross – coupled stiffness in addition to the direct one within the equations of motion. As demonstrated in Figure 2, at instant time $t = t_1$ the positioning of the springs with respect to the vertical axis (Y) is symmetric. While after Δt an asymmetric position occurs. As it will be shown in the next section, this asymmetrical configuration gives rise to varying stiffness which generates the parametric excitation within the system.
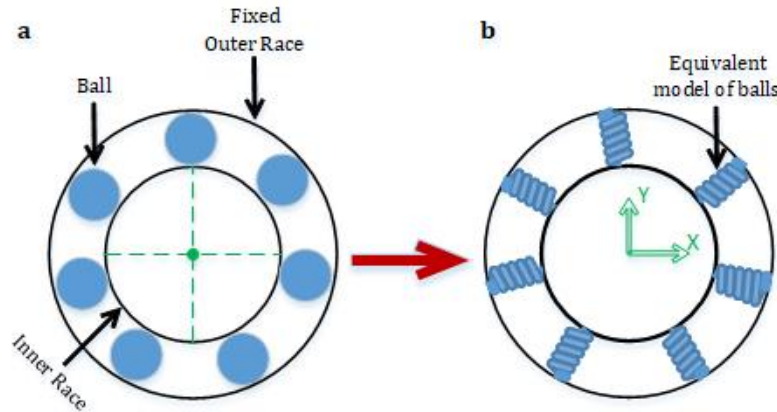

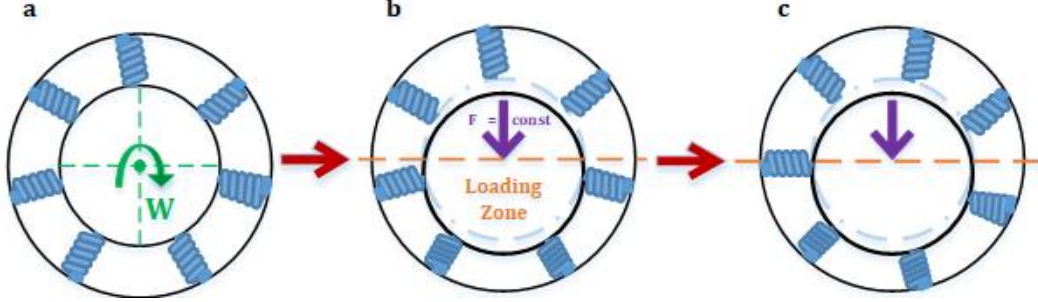**Figure 1: a)Bearing Model, b)Equivalent Bearing Model**

Figure 2: a) Rotating Configuration. b) Symmetric Configuration of the springs with respect to the vertical axis in the loading zone at $t = t_1$. c) Asymmetric positioning of the springs with respect to the vertical axis in the loading zone at $t = t_1 + \Delta t$

3. Governing equations of Motion

The bearing model and the related equations of motion have been extracted from the paper of Siranth et. al. [12]. In [12] the authors, starting from the bearing model of Figure 2a, used ANSYS to compute the diagram of the variable stiffness versus time. By performing the FFT they found that the main frequency component of the variable stiffness was at the frequency $q\omega$ where q is the number of the balls and ω the rotational speed. The bearing system is then modeled, as shown in Figure 3, as a simple mass – spring model with springs in the two main directions (x and y) and a coupling spring. All the springs have harmonically varying stiffness.

In [12] the equations of motion in the two directions x and are written as:

$$\frac{d^2x}{d\tau^2} + \zeta_1 \frac{dx}{d\tau} + [\delta_1 - \epsilon_1 \sin 2\tau]x + [\epsilon_2 \cos 2\tau]y = 0 \tag{1}$$

$$\frac{d^2y}{d\tau^2} + \zeta_2 \frac{dy}{d\tau} + [\delta_2 + \epsilon_3 \cos 2\tau]y + [\epsilon_4 \sin 2\tau]x = 0 \tag{2}$$

Where the parameters in Eq. (1) and Eq. (2) are dimensionless and are related to the physical parameters of the system:

$$2\tau = q\omega t \,, \delta_1 = \frac{4k_{xx}}{mq^2\omega^2} \,, \epsilon_1 = \frac{4k_x}{mq^2\omega^2} \tag{3}$$

$$\epsilon_2 = \frac{4k_{xy}}{mq^2\omega^2} \,, \delta_2 = \frac{4k_{yy}}{mq^2\omega^2} \,, \zeta_1 = \frac{2c_x}{q\omega m}$$

$$\epsilon_3 = \frac{4k_y}{mq^2\omega^2}, \epsilon_4 = \frac{4k_{yx}}{mq^2\omega^2} \,, \zeta_2 = \frac{2c_y}{q\omega m}$$

where q, ω and τ are the number of balls, rotational speed and time respectively. Considering Figure 3 k_{yy} and k_{xx} are the mean value of the direct stiffness in the horizontal and vertical direction. Here k_y , k_x and k_{xy} are the amplitude of the direct and cross – coupled stiffness at the qth harmonic and m, c_x and c_y are the mass and internal damping of the inner race. In this paper, it assumed the stiffness and the damping of the system in the horizontal and vertical directions are equal. Therefore, $\delta_1 = \delta_2, \epsilon_1 = \epsilon_3$. In addition, the cross – coupled stiffnesses are considered to be the same $\epsilon_2 = \epsilon_4$.

Eq. (1) and Eq. (2) are written in the form of a well – known parametrically excited equation the so – called Mathieu Equation. These equations can have stable or unstable solutions depending on the values of the parameters. The derivation of the stability and instability zones of the solution in the parameter space and the comparison of different methods for their derivation is discussed in the following section.
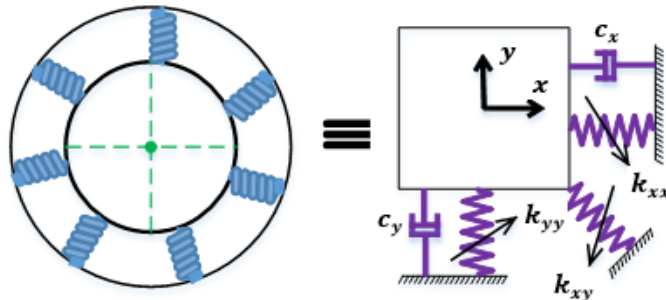
4. Floquet Theory

A well-known method for the determination of the stability and instability regions of the solutions of a Mathieu – like equation is the Floquet theory [2]. The Floquet theory is implemented with the following steps:

- The second order equations of motion (like equations (1) and (2)) are converted to first order differential equations using state space procedure;
- It is assumed an initial solution which is called fundamental solution in the form of

the identity matrix $I_{m \times m}$ (m is the number of the states);
- The Monodromy matrix is built [9] using time integration process during the time span of $[0, T]$
- Based on the eigenvalues of this matrix the nature (stable or unstable) of the response for each pair of parameters for example (δ, ϵ_1) is determined.

The value of the computed eigenvalues determines the stability or instability of the solution. In detail:

$\lambda_i \in \mathbb{R}$ with $\lambda_i \neq 1$	$|\lambda_i| = 1$	$\lambda_i \in \mathbb{C}$ with $|\lambda_i| \neq 1$	
$|\lambda_i| < 1 \rightarrow$ Stable behavior	$\lambda_i = 1 \rightarrow$ T periodic solutions	$|\lambda_i| > 1 \rightarrow$ Stable behavior	*(4)*
$|\lambda_i| > 1 \rightarrow$ Unstable behavior	$\lambda_i = -1 \rightarrow 2T$ periodic solutions	$|\lambda_i| < 1 \rightarrow$ Unstable behavior	

When the eigenvalues are repeated, the system is operating at the border between stability and instability regions. These regions can be depicted in a parameter space like the plane (δ, ϵ_1) ($\epsilon_2 = const$) in the form of stability boundary curves (SBC) which separates the stable from the unstable regions. The application of Floquet theory implies time integration of the equations of motion for each parameters set (δ, ϵ_1). The plot of the SBC curves using Floquet theory is then very time consuming. In the following sections, other approximate approaches are then proposed to obtain the same SBC curves. The Floquet theory is here applied at given points on the (δ, ϵ_1) plane solely as a reference for validation of the other methods.

5. Perturbation Method

The perturbation method is a semi – analytical very efficient approach to provide an approximate solution to the linear and weakly non – linear weakly damped governing equations of motion [8]. This method is based on a small parameter, the so – called Perturbation Parameter (usually represented by ϵ), which multiplies other parameters of the system. An equation in the perturbation form has two independent parameters: the Time t and the Perturbation Parameter ϵ. In order to proceed with this method, the following parameters must be first rescaled as follows:

$$\epsilon_1 = \epsilon \hat{\epsilon}_1 \qquad (5)$$
$$\epsilon_2 = \epsilon \hat{\epsilon}_2 \qquad (6)$$
$$\zeta = \epsilon \hat{\zeta} \qquad (7)$$

Substituting Eq. (5) to Eq. (7) in Eq. (1) and Eq. (2) the following is obtained:

$$\frac{d^2 x}{d\tau^2} + \epsilon \hat{\zeta} \frac{dx}{d\tau} + [\delta - \epsilon \hat{\epsilon}_1 \sin 2\tau]x + [\epsilon \hat{\epsilon}_2 \cos 2\tau]y = 0 \qquad (8)$$

$$\frac{d^2 y}{d\tau^2} + \epsilon \hat{\zeta} \frac{dy}{d\tau} + [\delta + \epsilon \hat{\epsilon}_1 \cos 2\tau]y + [\epsilon \hat{\epsilon}_2 \sin 2\tau]x = 0 \qquad (9)$$

In the following subsections, two of the main methods to solve perturbed equations are applied, the Multiple scale Methods (MSM) and the Harmonic Balance Method (HBM). Both methods allow to detect the resonance frequencies and the stability – instability SBC corresponding to a given resonance frequency. What should be mentioned is that when $\epsilon_2 \neq 0$ due to the complicated analysis procedure, this case is not studied by MSM while it is studied by HBM and addressed in section 6.3.

5.1. Multiple Scales Method (MSM)

This method is just applied for the case when the equations are uncoupled ($\epsilon_2 = 0$). In this section, the responses of the system are approximated based on slow and fast time scales which are defined as follows:

$$T_0 = \tau \qquad (10)$$
$$T_1 = \epsilon \tau \qquad (11)$$

The time derivatives are written in terms of the new time scales, this leads to the transformation of ordinary differential equations in partial differential equations. The new time derivatives are:

$$\frac{d}{d\tau} = D_0 + \epsilon D_1 + \cdots \qquad (12)$$

$$\frac{d^2}{d\tau^2} = D_0^2 + 2\epsilon D_0 D_1 + \cdots \qquad (13)$$

where $D_i = \partial/\partial T_i$

Substituting Eq. (12) and Eq. (13) in Eq. (8) and Eq. (9) results in the followings:

$$D_0^2 x_0 + \delta x_0$$
$$+ \epsilon\big(D_0^2 x_1 + \delta x_1 + 2D_0 D_1 x_0 + \hat{\zeta} D_0 x_0 \qquad (14)$$
$$- \hat{\epsilon}_1 x_0 \sin 2T_0\big) = 0$$

$$D_0^2 y_0 + \delta y_0$$
$$+ \epsilon\big(D_0^2 y_1 + \delta y_1 + 2D_0 D_1 y_0 + \hat{\zeta} D_0 y_0 \qquad (15)$$
$$+ \hat{\epsilon}_1 y_0 \cos 2T_0\big) = 0$$

The next step consists in equating the coefficients of each power of ϵ. The following equations are obtained:

$$D_0^2 x_0 + \delta x_0 = 0 \rightarrow x_0 = A_1(T_1)\cos\sqrt{\delta}T_0 + B_1(T_1)\sin\sqrt{\delta}T_0 \qquad (16)$$

$$D_0^2 y_0 + \delta y_0 = 0 \rightarrow y_0 = A_2(T_1)\cos\sqrt{\delta}T_0 + B_2(T_1)\sin\sqrt{\delta}T_0 \qquad (17)$$

$$D_0^2 x_1 + \delta x_1 = -2D_0 D_1 x_0 - \hat{\zeta} D_0 x_0 + \hat{\epsilon}_1 x_0 \sin 2T_0 \rightarrow D_0^2 x_1 + \delta x_1$$
$$= -2\sqrt{\delta}\left(-\frac{\partial A_1}{\partial T_1}\sin\sqrt{\delta}T_0 + \frac{\partial B_1}{\partial T_1}\cos\sqrt{\delta}T_0\right) - \hat{\zeta}\sqrt{\delta}\left(-A_1\sin\sqrt{\delta}T_0 + B_1\cos\sqrt{\delta}T_0\right) \qquad (18)$$
$$+ \frac{\hat{\epsilon}_1}{2}\big(A_1[\sin(\sqrt{\delta}+2)T_0 - \sin(\sqrt{\delta}-2)T_0] + B_1[\cos(\sqrt{\delta}+2)T_0 - \cos(\sqrt{\delta}-2)T_0]\big)$$

$$D_0^2 y_1 + \delta y_1 = -2D_0 D_1 y_0 - \hat{\zeta} D_0 y_0 - \hat{\epsilon}_1 y_0 \cos 2T_0 \rightarrow D_0^2 y_1 + \delta y_1$$
$$= -2\sqrt{\delta}\left(-\frac{\partial A_2}{\partial T_1}\sin\sqrt{\delta}T_0 + \frac{\partial B_2}{\partial T_1}\cos\sqrt{\delta}T_0\right) - \hat{\zeta}\sqrt{\delta}\left(-A_2\sin\sqrt{\delta}T_0 + B_2\cos\sqrt{\delta}T_0\right) \qquad (19)$$
$$- \frac{\hat{\epsilon}_1}{2}\big(A_2[\cos(\sqrt{\delta}+2)T_0 + \cos(\sqrt{\delta}-2)T_0] + B_2[\sin(\sqrt{\delta}+2)T_0 + \sin(\sqrt{\delta}-2)T_0]\big)$$

Eq. (16) and Eq. (17) are ordinary differential equations with the solution x_0 and y_0 written on the same row on the right. It is well known, from the literature [7], that the first bolded terms in Eq. (18) and Eq. (19) are the so – called "secular term generator" while the terms with $(\sqrt{\delta}-2)$ will generate terms in x_1 and y_1 where the denominator is called small – divisor.

The term δ, according to Lindstedt – Poincare' method where perturbed terms can alter the resonance frequency, could be rewritten and expanded as follows:

$$\delta = \delta_0 + \epsilon\delta_1 + O(\epsilon^2) \qquad (20)$$

In Eq. (20) δ_0 can be any value of resonance frequency. Here $\delta_0 = 1$. Replacing δ by its new form in Eq. (18) and Eq. (19) and equating to zero the secular term generators, results in the following expression:

$$\dot{\vec{X}}$$

$$= \begin{bmatrix} -\hat{\zeta} - \dfrac{\hat{\epsilon}_1}{2} & \delta_1 & 0 & 0 \\[2mm] -\delta_1 & -\hat{\zeta} - \dfrac{\hat{\epsilon}_1}{2} & 0 & 0 \\[2mm] 0 & 0 & -\delta_1 - \dfrac{\hat{\epsilon}_1}{2} & -\hat{\zeta} \\[2mm] 0 & 0 & -\hat{\zeta} & \delta_1 - \dfrac{\hat{\epsilon}_1}{2} \end{bmatrix} \vec{X} \qquad (21)$$

$$[A]$$

Where $\vec{X} = \{A_1, B_1, A_2, B_2\}'$. Equation (21) is a system of first order linear differential equations, with a solution of the form $\vec{X} = \vec{K}e^{\gamma t}$ that substituted in (21) results in the following eigenvalue – eigenvector problem:

$$\gamma\vec{K} = A\vec{K} \qquad (22)$$

It is then necessary to compute the eigenvalues of matrix A to discuss the stability of the solutions. The eigenvalues of A are:

$$\gamma_{1,2} = -\frac{\hat{\epsilon}_1}{2} \pm \sqrt{\delta_1^2 + \hat{\zeta}^2} \qquad (23)$$

5

$$\gamma_{3,4} = -\left(\hat{\zeta} + \frac{\hat{\epsilon}_1}{2}\right) \pm i\sqrt{\delta_1^2}$$

From (3) $\epsilon_1 > 0$, therefore, the solutions which are concerned with $\gamma_{3,4}$ are always stable. On the other hand, the solutions related to $\gamma_{1,2}$ might be stable or unstable. Since along the stability boundary curves (SBC) the responses are periodic with $2T$ period (Here $T = \pi$), in order to obtain the SBC equations, it is necessary to put the eigenvalues $\gamma_{1,2}$ equal to zero:

$$-\frac{\hat{\epsilon}_1}{2} \pm \sqrt{\delta_1^2 + \hat{\zeta}^2} = 0 \rightarrow \delta_1$$
$$= \pm\sqrt{\frac{\hat{\epsilon}_1^2}{4} - \hat{\zeta}^2} \qquad (24)$$

Substituting Eq. (24) in Eq. (20), the SBC equations corresponding to the resonance frequency of $\delta_0 = 1$ can be obtained:

$$\delta = 1 \pm \sqrt{\frac{\epsilon_1^2}{4} - \zeta^2} + \cdots \qquad (25)$$

In the following section, the method of harmonic balance as another approximate approach to obtain the same SBCs is adopted.

6. Harmonic Balance Method (HBM)

Unlike MSM, which provides not only the SBC but also the solution in the vicinity of the curves themselves, HBM solely focuses on the SBC. However, one advantage of HBM is that, by simply increasing the number of harmonics, one is able to compute additional resonance frequencies and as a result more SBCs at a minimal additional computational cost. The corresponding MSM computational effort is much larger. According to Floquet theory when $\epsilon_2 = 0$, the responses along the SBCs are periodic with T or $2T$. In the current problem $T = \pi$. The general form of the responses applying HBM is considered as below:

$$x(t)$$
$$= a_0 + \sum_{n=1}^{N}(a_n \cos n\omega_s\tau + b_n \sin n\omega_s\tau)$$
$$y(t) \qquad\qquad (26)$$
$$= c_0 + \sum_{n=1}^{N}(c_n \cos n\omega_s\tau + d_n \sin n\omega_s\tau)$$

Where N is the number of the harmonics which in this paper is equal to 2. In addition

$$\omega_s = \frac{2\pi}{T'} \qquad (27)$$

Where T' is the period of the response. Setting Eq. (26) and Eq. (27) in the equations of motion and considering Floquet theory, the SBCs corresponding to the resonance frequencies could be obtained. To do so, the following two cases are taken into account.

6.1. Π Response ($T' = T = \pi \ \omega_s = 2$)
In this case, the responses would be as follows:

$$x = a_0 + a_1 \cos 2\tau + b_1 \sin 2\tau + a_2 \cos 4\tau + b_2 \sin 4\tau$$
$$y = c_0 + c_1 \cos 2\tau + d_1 \sin 2\tau + c_2 \cos 4\tau + d_2 \sin 4\tau \qquad (28)$$

Substituting them in the Eq. (1) and Eq. (2) and balancing the resulted equations would be organized in the following matrix form:

$$[B_\pi]\{x_\pi\} = 0 \qquad (29)$$

Where matrix B_π and vector x_π are presented by eq. (A1) in the appendix. For nontrivial equation it is required to set:

$$|B_\pi| = 0 \qquad (30)$$

Where the numerical computation of Eq. (30) gives the SBC corresponding to π responses.

6.2. 2Π Response ($T' = T = 2\pi \ \omega_s = 1$)
The responses in Eq. (28) would be expanded as follows:

$$x$$
$$= a_1 \cos \tau + b_1 \sin \tau + a_3 \cos 3\tau + b_3 \sin 3\tau$$
$$y \qquad\qquad (31)$$
$$= c_1 \cos \tau + d_1 \sin \tau + c_3 \cos 3\tau + d_3 \sin 3\tau$$

It should be noted that $\cos 2\tau$ and $\sin 2\tau$ are neglected in the current case since their minimum period is π which has previously been considered. Here also the zeroth harmonics (Terms corresponding to a_0 and c_0) which have already been taken into account in section 6.1 are neglected. Following the same procedure as before, the subsequent matrix – vector form of the equations due to balancing procedure is be obtained:

$$[B_{2\pi}]\{x_{2\pi}\} = 0 \qquad (32)$$

Where $B_{2\pi}$ and $x_{2\pi}$ are presented by Eq. (A2). Nontrivial solutions can be obtained if:

$$|B_{2\pi}| = 0 \qquad (33)$$

Where the numerical computation of Eq. (33) gives the SBC corresponding to 2π responses.

6.3. Responses for $\epsilon_2 > 0$

In the presence of coupling, the <u>dominant frequencies</u> of the solutions are neither 2π nor π. According to [15] the dominant frequencies are ω_1 and ω_2. The characteristics of these frequencies are as follows:

- Their summation is equal to forcing frequency which is 2 (the frequency of parametric exciter from Eq. (8) and (9))
- They vary when either ϵ_1 or ϵ_2 change.

As shown in [15] multi-DOFs coupled systems are interested by primary resonances (occurring at ω_1 and ω_2) and by a combination resonance, i.e. occurring in the neighborhood of the frequency $\omega_1 + \omega_2$. The present work focuses on the combination resonance since, as stated in [14], in the case of coupled multi-DOFs systems the combination resonance causes the largest instability region and is most often encountered.

Using the first characteristic, one can write one of the frequencies as a function of the other one

$$\omega_2 = \omega_{px} - \omega_1 \tag{34}$$

Where $\omega_{px} = 2$ is the forcing frequency. Now, the responses should be approximated in terms of the dominant frequencies as follows:

$$\begin{aligned}
x &= a_1 \cos \omega_1 \tau + b_1 \sin \omega_1 \tau \\
&+ a_2 \cos(\omega_{px} - \omega_1)\tau \\
&+ b_2 \sin(\omega_{px} - \omega_1)\tau \\
y &= c_1 \cos \omega_1 \tau + d_1 \sin \omega_1 \tau \\
&+ c_2 \cos(\omega_{px} - \omega_1)\tau \\
&+ d_2 \sin(\omega_{px} - \omega_1)\tau
\end{aligned} \tag{35}$$

Replacing Eq. (35) by their corresponding terms within the equations of motion and proceeding as before (Balancing procedure), the final form of the equations of balancing could be summarized as below:

$$[B]\{x\} = 0 \tag{36}$$

Where $[B]$ and $\{x\}$ are represented by Eq. (A3) in the appendix. For non – trivial solution it is necessary to set

$$|B| = 0 \tag{37}$$

Unlike previous cases, where δ was the only unknown, now ω_1 is also an unknown. In order to compensate for the deficiency of the equations, the maximum minor of $[B]$ should be equated to zero [6]. Since due to Eq. (37)

one of the constants of vector $\{x\}$ becomes arbitrary, by putting the maximum minor of $[B]$ equal to zero – no matter which column and row are eliminated – another parameter of the vector of constants is considered arbitrary. Since, $[B]$ is 8×8, hence the corresponding highest minor would be 7×7 and would be presented as $[B]_m$. Therefore, the extra equation needed to determine all unknowns can be derived by:

$$|B|_m = 0 \tag{38}$$

Finally, solving Eq. (37) and Eq. (38) together, the resultant SBCs would be acquired.

7. Results and Discussions

In this section the numerical results acquired by Floquet Theory, MSM and HBM are presented and discussed. The section is divided into three sub – sections corresponding to three cases 1) Uncoupled – Undamped system, 2) Uncoupled – Damped system and 3) Coupled – damped system respectively. In each sub – section the SBCs obtained through the approximate methods are shown on the (δ, ϵ_1) plane ($\epsilon_2 = const$). A few selected results from the Floquet theory are presented as a reference for validation. In addition, in some cases, time integration is used to classify different regions of the (δ, ϵ_1) (on different sides of a SBC) as either Stable or Unstable.

7.1. Case 1: Uncoupled – Undamped System

The SBC emanating from $\delta = 1$ and obtained using the first order expansion MSM are shown in Figure 4 using a red dashed line. Considering these curves, the plane can be divided into three different regions: inside the curve, on the curve and outside the curve. Unstable and stable regions are indicated by letters U and S on the plane of the SBCs. The inside area is so – called an Unstable region where the system experiences divergent and exponentially growing responses as time passes. This is further confirmed by the Time response of Point 3 in Figure 5 where it is evident that x and y responses are increasing drastically. Proceeding further and investigating the points on the curves, the accuracy of the MSM for predicting the SBC is confirmed by Floquet Theory. Figure 6 shows the magnitude of the eigenvalues of the monodromy matrix as a function of parameters (δ, ϵ_1). As mentioned in Section 4, when the absolute value of the eigenvalues of

the monodromy matrix is equal to one, the solutions are periodic, in the present case with period π or 2π. Correspondingly these are the points which are located on the SBCs. According to Figure 6a, the intersection of the $|\lambda| = 1$ lines with the blue curves representing the eigenvalues of the monodromy matrix for different values of (δ, ϵ_1) correspond to points belonging to the SBCs. The reader will notice that the coordinates of these points in Figure 6a coincide with those belonging to the SBC shown in Figure 4. As presented below these points are termed A1 & D1 when $\epsilon_1 = 0.6$ and B1 & C1 when $\epsilon_1 = 0.4$. Furthermore, in order to verify the nature of the responses on the SBC the time integration of the A1 and D1 is carried out and shown in Figure 5. As predicted by the Floquet Theory, the time responses on the SBC are periodic. If one chooses parameters outside the SBCs, all resulting responses are stable and bounded. To show this, the time responses of points 1 and 2 from Figure 4 are shown in Figure 5. The reader will notice that both the responses in x and y directions are bounded as time progresses. Although by applying MSM one can acquire the SBCs rather accurately, there are two main drawbacks to this method. Firstly, it is not clear what kind of solutions (periodic with π or 2π) lie on the SBC emanated from $\delta = 1$ without resorting to time integration. Secondly, no information is given on the SBCs resulting from other resonance frequencies. In order to overcome these drawbacks, HBM, a frequency – domain

based approximate method is utilized. According to Figure 4, the SBC emanated from $\delta = 0$ is obtained by considering the zeroth harmonic within the approximation of the responses. The area under this curve is unstable. The SBCs which are emanating from $\delta = 1$ perfectly match those acquired by MSM. As mentioned in Section 6, these curves are associated with 2π solutions. To show this the FFT diagram of the points A1 and D1 in Figure 5. To show this, the FFT diagram of points A1 and D1 are presented in Figure 5. According to these plots the dominant frequency is equal to $1/2\pi$. It should be mentioned that spurious components close to $1/2\pi$ are present due the difficulty of selecting a (δ, ϵ_1) combination which is exactly on the SBC. Another SBC which is obtained using this method is the one emanating from the resonance frequency $\delta = 4$. According to Floquet Theory, the solutions which lie on these curves are periodic with π corresponding to $\lambda = -1$. In order also to investigate the accuracy of this predicted curve the Floquet theory is applied. The result is presented in Figure 6b for $\epsilon_1 = 0.8$. Locating the position of intersecting points (E1 & F1) on the $|\lambda| = 1$ line on the (δ, ϵ_1) plane, the validity of Eq. (28) and Eq. (31) is confirmed. Furthermore, the higher the resonance the narrower the SBCs and therefore the unstable areas. This means that a sound design check should not overlook the first two resonances.
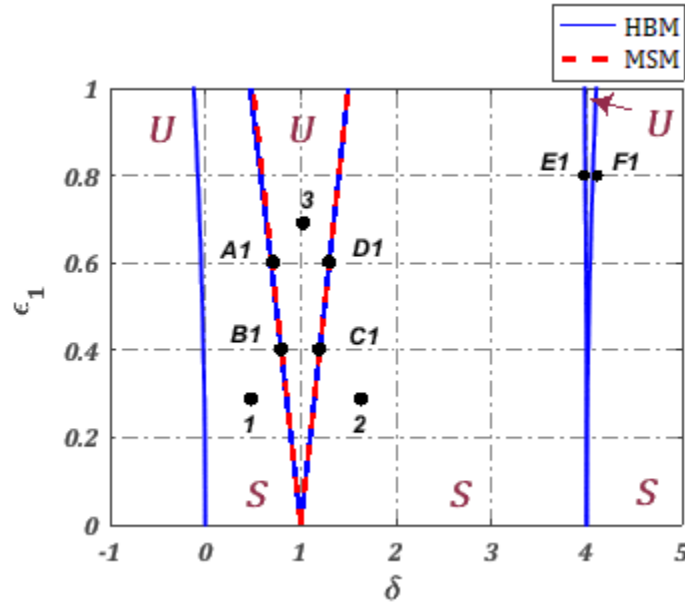
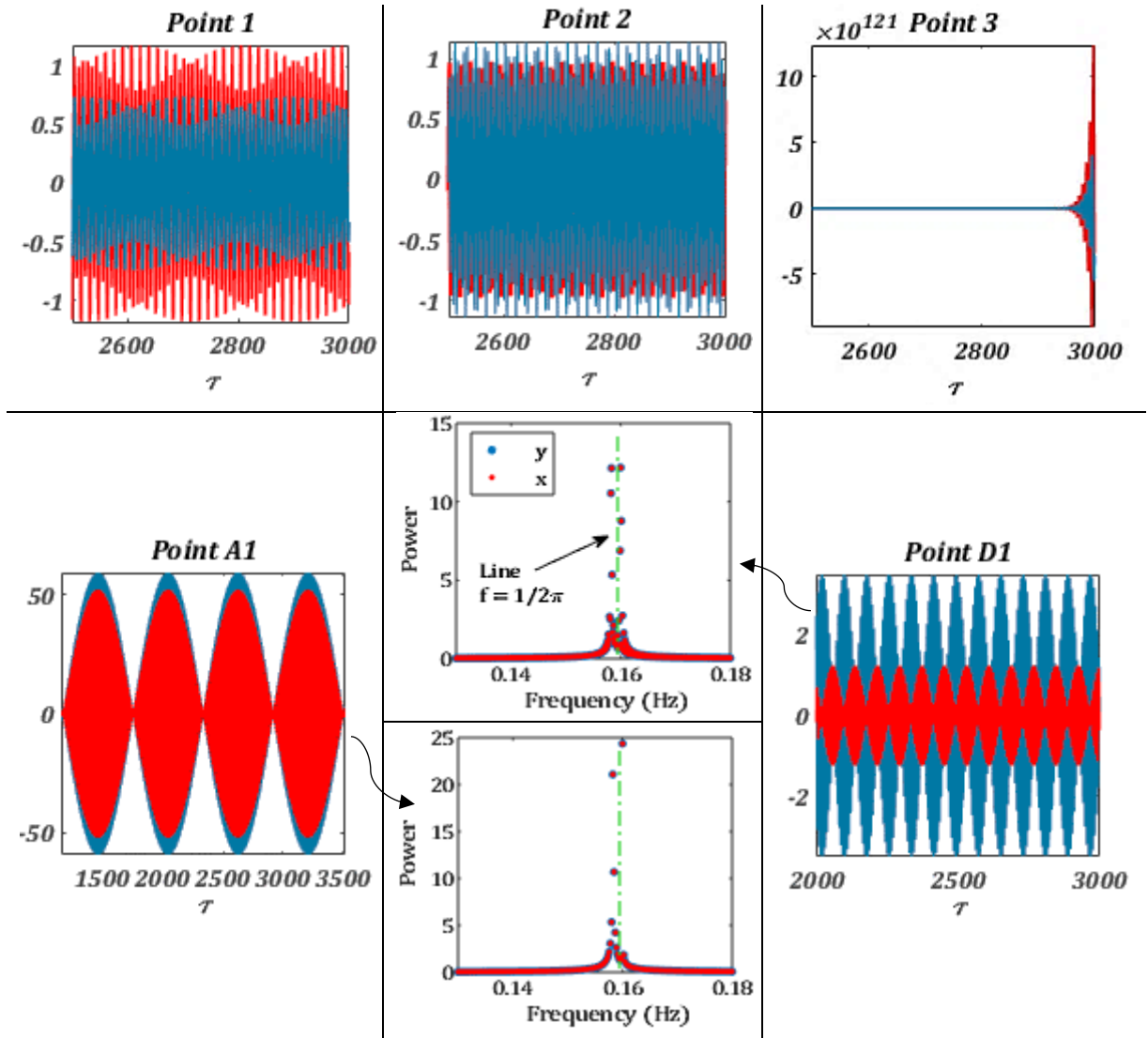**Figure 4: Stability boundary curves for the undamped – uncoupled system $(\zeta = 0 , \epsilon_2 = 0)$**

Figure 5: Time responses related to the points of SBC diagram for the undamped – uncoupled bearing system (x ——, y ——) and FFT of the point A1 & D1
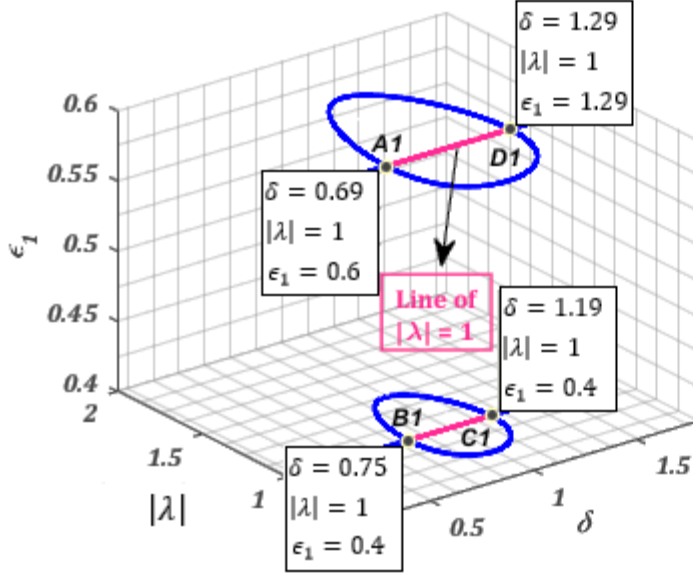
Figure 6a: The points on the SBCs using Floquet Theory for undamped – uncoupled system for $\epsilon_1 = 0.4$ and $\epsilon_1 = 6$

Figure 6b: The points on the SBCs using Floquet Theory for undamped – uncoupled system for $\epsilon_1 = 0.8$

7.2. Case 2: Uncoupled - Damped System

In this section, the influence of damping on the stability of the system is investigated. As has been observed from case 1, the results obtained through HBM and MSM match. It is here chosen, in order to avoid an excessive number of figures, to show only the results obtained through HBM. As shown in Figure 7, the $\delta = 0$ curve maintains its trend (compare with Figure 4) but with a slight inward bend, thus increasing the size of the stable area. As for the $\delta = 1$ curve, pertaining to the 2π solution, it can be seen that the presence of damping shifts the origin of the curve. The SBC starts at $\epsilon_1 = 0$ and $\delta = 1$ if no damping is present, while it moves up as soon as the ζ parameter increases. Another effect of a non-null ζ value is the curvature of the SBC. In fact,
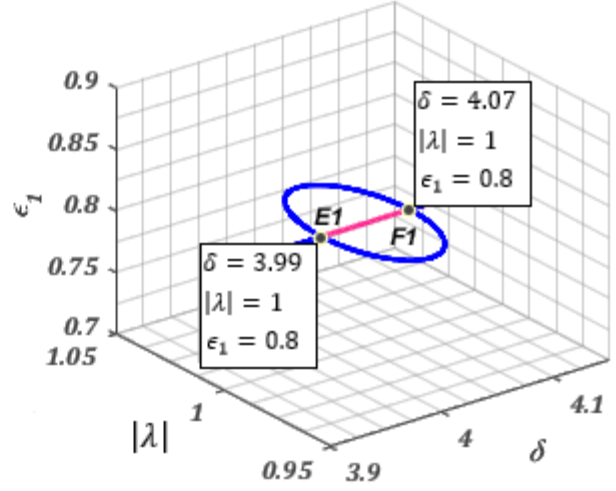
by considering the damping within the system the area of instability (inside the SBCs) is decreasing and on the other hand, the stable region is growing (outside the SBCs). Another feature which may catch the reader's attention is the presence of sequential points on the $\delta = 1$ line. In order to determine the nature of these points, two of them are randomly selected and their time responses are presented in Figure 8. Considering the time responses, all points are completely stable. In order to offer further proof of the accuracy of the SBCs, the Floquet is applied for the case of $\zeta = 0.01$. According to the intersections of the $|\lambda| = 1$ line with the eigenvalues line are points A2 & D2 for $\epsilon_1 = 0.6$ and points. B2 & C2 for $\epsilon_1 = 0.4$. This set of results matches those observed in Figure 7. The Floquet – based results for this case are not shown for brevity.
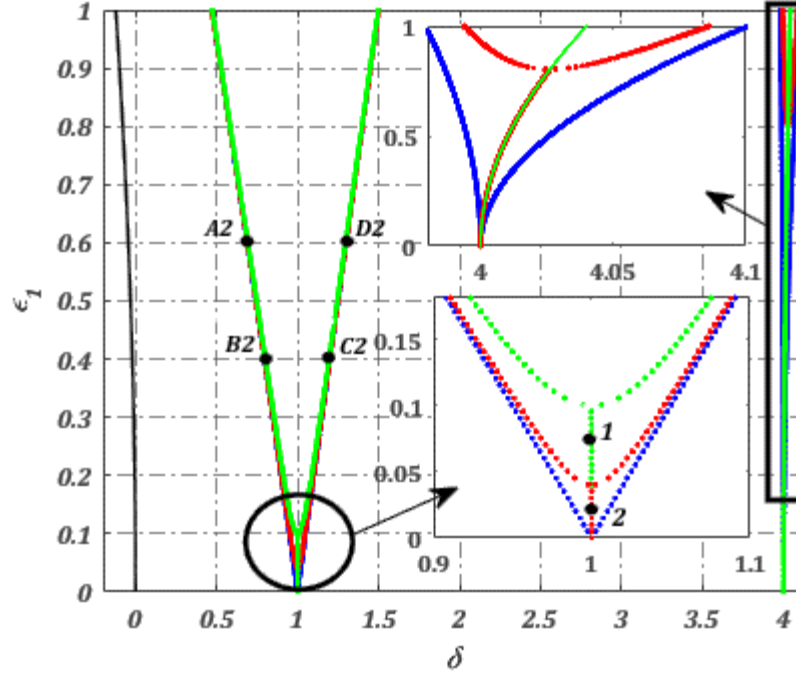
10

Figure 7: stability boundary curves obtained by HBM for the damped – uncoupled system ($\epsilon_2 = 0, \zeta = 0 , \zeta = 0.01 , \zeta = 0.05$)
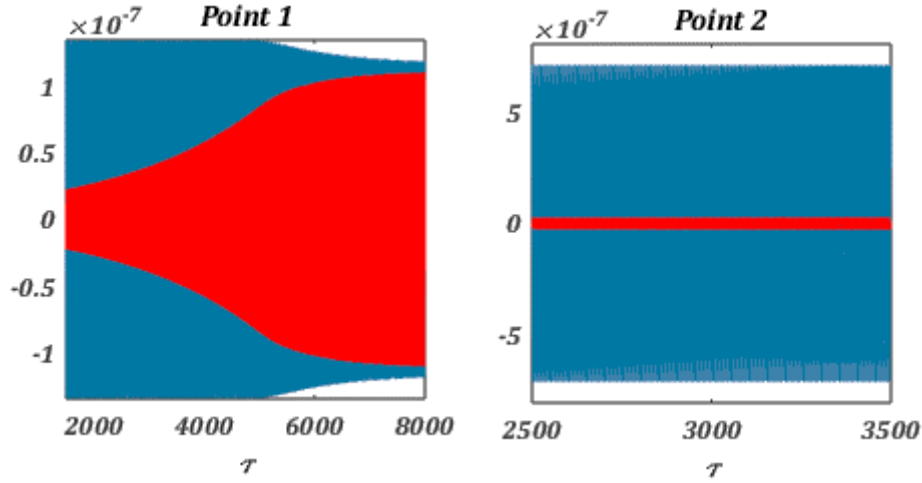

Figure 8: Time response (x ——, y ——)

7.3. Case 3: Coupled – Damped System

In this section, a realistic general model of a bearing system is considered. The coupling variable ϵ_2 is therefore non-null. Figure 9 shows the corresponding SBCs obtained using HBM. It is shown how the presence of the cross – coupling detaches the $\delta = 1$ curves, thus increasing the instability area. Once again coordinates of selected points on the SBC curves match those found at the intersection of

the curve representing the eigenvalues of the monodromy matrix and $|\lambda| = 1$. Although the SBCs obtained for this case appear to be accurate, there are some curves which relate to unacceptable (non-physical) values of dominant frequencies and should therefore be eliminated. In Figure 9 the undesirable curves are shown in different colors and labeled according to the reason which makes them

unacceptable. In detail, the blue curves are the result of equal dominant frequencies $\omega_1 = \omega_2$. As mentioned in Section 6.3, for the coupled case, the summation of the dominant frequencies equals to the forcing frequency π. If $\omega_1 = \omega_2$ it would mean that the frequency of the solutions is $\omega = \omega_1 = \omega_2 = 2$; however, due to the cross – coupling such solutions do not exist and therefore, they have been ignored. Another curve which is not of interest is the red one. As depicted in Figure 9, this curve is neglected due to the negative values of dominant frequencies. The last neglected curves are the ones shown in pink, whose corresponding frequencies are complex with a positive real part. The Floquet – based analysis of this case is presented in Figure 10. With reference to this figure, the reader will notice that point A3 is missing because no intersection between the line of unit eigenvalues and other eigenvalues is present. Having eliminated the unacceptable curves, the final SBCs related to the damped coupled system can be plotted as in Figure 11. In order to detect the stable and unstable regions, some random points are selected and their corresponding time responses are computed. In Figure 11, the stable points outside the SBCs are shown in purple. On the other hand, the inner areas see an unstable response and the corresponding points are depicted in red.
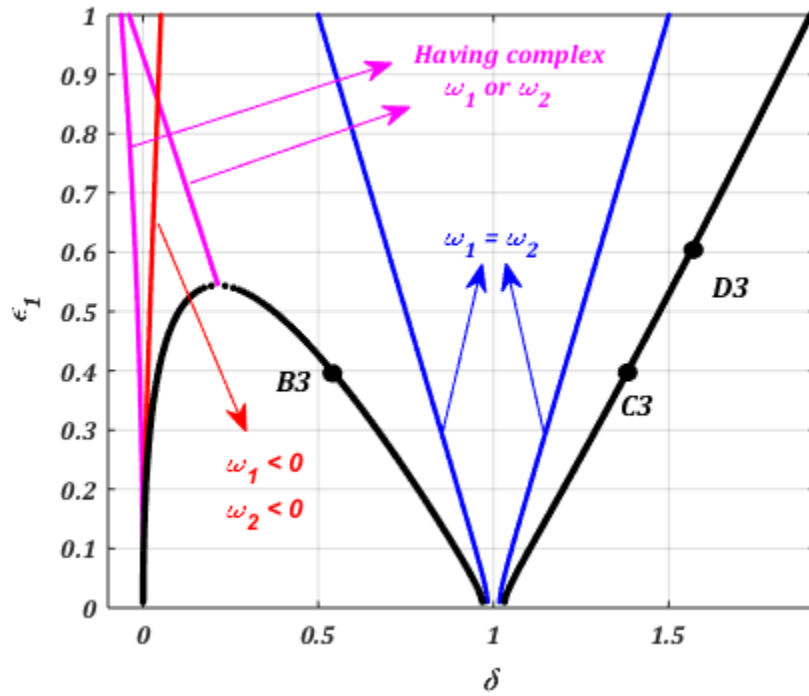

Figure 9: Stability boundary curves obtained by HBM and the Unacceptable Frequencies for the damped – coupled system ($\zeta = 0.01, \epsilon_2 = 0.05$)
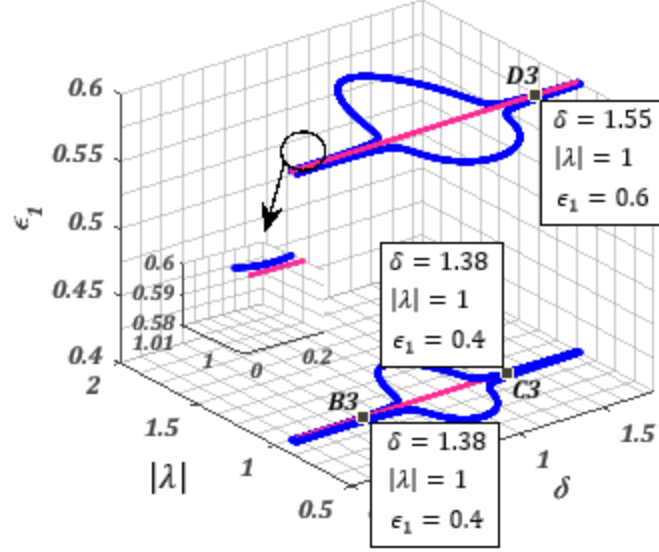
Figure 10: The points on the TCs using Floquet Theory for damped – coupled system with $\zeta = 0.01, \epsilon_2 = 0.05$ amd for $\epsilon_1 = 0.4$ and $\epsilon_1 = 0.6$
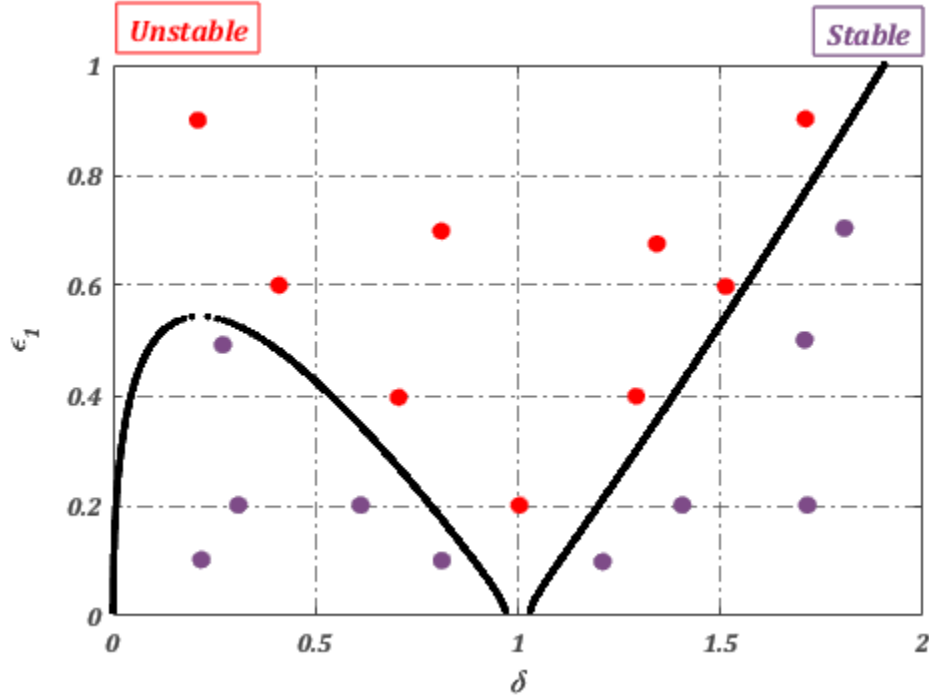

Figure 11: Final SBC for coupled – damped system ($\zeta = 0.01, \epsilon_2 = 0.05$)

8. Conclusion

This paper applies a series of approximate methods, namely Multiple Scales and Harmonic Balance, to perform the stability analysis of a bearing system. Stability analysis of bearing systems is typically carried out using costly time marching techniques. The objective is to obtain the stability boundary curves in the 3D input parameter space at an affordable computational cost. These curves can become a powerful design tool as they provide the designer with a full picture of the influence that changes in the bearing geometry and rotational speed have on the system stability. Based on the results' analysis the following observations are made:

13

- A preliminary case (uncoupled – undamped) is here used as a demonstrator. The results of MSM and HBM are not only in line with each other but also are compatible with Floquet Theory, here used as a validation reference.
- In the presence of the damping, the stability regions increase.
- If coupling between the two degrees of freedom of the bearing is considered, the SBCs change their shape and the unstable regions expand. An ad-hoc Harmonic Balance procedure has been developed to correctly capture the SBCs morphology, its results confirmed by Floquet and Time integration.
- As far as approximate methods go, the authors found Harmonic Balance to be more convenient than Multiple Scales, especially if the user is interested in higher resonance frequencies and/or if the number of dominant harmonics is larger than one (Coupled – Damped bearing system)

9. Appendix

$$
\begin{bmatrix}
\delta & 0 & -\dfrac{\epsilon_1}{2} & 0 & 0 & 0 & \dfrac{\epsilon_2}{2} & 0 & 0 & 0 \\
0 & \delta-4 & 2\zeta & 0 & -\dfrac{\epsilon_1}{2} & \epsilon_2 & 0 & 0 & \dfrac{\epsilon_2}{2} & 0 \\
-\epsilon_1 & -2\zeta & \delta-4 & \dfrac{\epsilon_1}{2} & 0 & 0 & 0 & 0 & 0 & \dfrac{\epsilon_2}{2} \\
0 & 0 & \dfrac{\epsilon_1}{2} & \delta-16 & 4\zeta & 0 & \dfrac{\epsilon_2}{2} & 0 & 0 & 0 \\
0 & -\dfrac{\epsilon_1}{2} & 0 & -4\zeta & \delta-16 & 0 & 0 & \dfrac{\epsilon_2}{2} & 0 & 0 \\
0 & 0 & \dfrac{\epsilon_2}{2} & 0 & 0 & \delta & \dfrac{\epsilon_1}{2} & 0 & 0 & 0 \\
0 & 0 & 0 & 0 & \dfrac{\epsilon_2}{2} & \epsilon_1 & \delta-4 & 2\zeta & \dfrac{\epsilon_1}{2} & 0 \\
\epsilon_2 & 0 & 0 & -\dfrac{\epsilon_1}{2} & 0 & 0 & -2\zeta & \delta-4 & 0 & \dfrac{\epsilon_1}{2} \\
0 & 0 & -\dfrac{\epsilon_2}{2} & 0 & 0 & 0 & \dfrac{\epsilon_1}{2} & 0 & \delta-16 & 4\zeta \\
0 & \dfrac{\epsilon_2}{2} & 0 & 0 & 0 & 0 & 0 & \dfrac{\epsilon_1}{2} & -4\zeta & \delta-16
\end{bmatrix}
\begin{Bmatrix} a_0 \\ a_1 \\ b_1 \\ a_2 \\ b_2 \\ c_0 \\ c_1 \\ d_1 \\ c_2 \\ d_2 \end{Bmatrix} = \{\vec{0}\}
\tag{A1}
$$

$$
\begin{bmatrix}
\delta-1 & \zeta-\dfrac{\epsilon_1}{2} & 0 & -\dfrac{\epsilon_1}{2} & \dfrac{\epsilon_2}{2} & 0 & \dfrac{\epsilon_2}{2} & 0 \\
-\left(\zeta+\dfrac{\epsilon_1}{2}\right) & \delta-1 & \dfrac{\epsilon_1}{2} & 0 & 0 & -\dfrac{\epsilon_2}{2} & 0 & \dfrac{\epsilon_2}{2} \\
0 & \dfrac{\epsilon_1}{2} & \delta-9 & 3\zeta & \dfrac{\epsilon_2}{2} & 0 & 0 & 0 \\
-\dfrac{\epsilon_1}{2} & 0 & -3\zeta & \delta-9 & 0 & \dfrac{\epsilon_2}{2} & 0 & 0 \\
0 & \dfrac{\epsilon_2}{2} & 0 & \dfrac{\epsilon_2}{2} & \delta-1+\dfrac{\epsilon_1}{2} & \zeta & \dfrac{\epsilon_1}{2} & 0 \\
\dfrac{\epsilon_2}{2} & 0 & -\dfrac{\epsilon_2}{2} & 0 & -\zeta & \delta-1-\dfrac{\epsilon_1}{2} & 0 & \dfrac{\epsilon_1}{2} \\
0 & -\dfrac{\epsilon_2}{2} & 0 & 0 & \dfrac{\epsilon_1}{2} & 0 & \delta-9 & 3\zeta \\
\dfrac{\epsilon_2}{2} & 0 & \dfrac{\epsilon_1}{2} & 0 & 0 & 0 & -3\zeta & \delta-9
\end{bmatrix}
\begin{Bmatrix} a_1 \\ b_1 \\ a_3 \\ b_3 \\ c_1 \\ d_1 \\ c_3 \\ d_3 \end{Bmatrix} = \{\vec{0}\}
\tag{A2}
$$

$$
\begin{bmatrix}
\delta - \omega_1^2 & \zeta\omega_1 & 0 & -\dfrac{\epsilon_1}{2} & 0 & 0 & \dfrac{\epsilon_2}{2} & 0 \\[2mm]
-\zeta\omega_1 & \delta - \omega_1^2 & -\dfrac{\epsilon_1}{2} & 0 & 0 & 0 & 0 & -\dfrac{\epsilon_2}{2} \\[2mm]
0 & -\dfrac{\epsilon_1}{2} & \delta - (\omega_{px}-\omega_1)^2 & \zeta(\omega_{px}-\omega_1) & \dfrac{\epsilon_2}{2} & 0 & 0 & 0 \\[2mm]
-\dfrac{\epsilon_1}{2} & 0 & -\zeta(\omega_{px}-\omega_1) & \delta - (\omega_{px}-\omega_1)^2 & 0 & -\dfrac{\epsilon_2}{2} & 0 & 0 \\[2mm]
0 & 0 & 0 & \dfrac{\epsilon_2}{2} & \delta - \omega_1^2 & \zeta\omega_1 & \dfrac{\epsilon_1}{2} & 0 \\[2mm]
0 & 0 & \dfrac{\epsilon_2}{2} & 0 & -\zeta\omega_1 & \delta - \omega_1^2 & 0 & -\dfrac{\epsilon_1}{2} \\[2mm]
0 & \dfrac{\epsilon_2}{2} & 0 & 0 & \dfrac{\epsilon_1}{2} & 0 & \delta - (\omega_{px}-\omega_1)^2 & \zeta(\omega_{px}-\omega_1) \\[2mm]
\dfrac{\epsilon_2}{2} & 0 & 0 & 0 & 0 & -\dfrac{\epsilon_1}{2} & -\zeta(\omega_{px}-\omega_1) & \delta - (\omega_{px}-\omega_1)^2
\end{bmatrix}
\begin{Bmatrix} a_1 \\ b_1 \\ a_2 \\ b_2 \\ c_1 \\ d_1 \\ c_2 \\ d_2 \end{Bmatrix} = \{\vec{0}\} \qquad (A3)
$$

References

[1] H. Cao, L. Niu, S. Xi, X Chen, Mechanical model development of rolling bearing-rotor systems: A review, Journal of Mechanical Systems and Signal Processing, (2018) 102: 37 – 58

[2] J. Metsebo, N. Upadhyay, P. K. Kankar, B. R. Nana Nbendjo, Modelling of a rotor-ball bearings system using Timoshenko beam and effects of rotating shaft on their dynamics. Journal of Mechanical Science and Technology (2016) 30: 5339 – 5350

[3] S.P. Harsha, Non-linear dynamic response of a balanced rotor supported on rolling element bearings using Timoshenko beam and effects of rotating shaft on their dynamics, Journal of Mechanical Science and Technology (2016) 30: 5339 – 5350

[4] V. Vakharia, V.K. Gupta, P.K. Kankar, Nonlinear Dynamic Analysis of Ball Bearings Due to Varying Number of Balls and Centrifugal Force, Conference on Rotor Dynamics, Mechanisms and Machine Science 21, Springer International Publishing Switzerland (2015) 1831 : 1840

[5] Changqing Bai, Hongyan Zhang, Qingyu Xu, Subharmonic resonance of a symmetric ball bearing–rotor system, International Journal of Non-Linear Mechanics (2013) 50: 1–10

[6] K. De Moerlooze, F. Al-Bender, H. Van Brussel, Modeling of the dynamic behavior of systems with rolling elements, International Journal of Non-Linear Mechanics (2011) 46: 222–233

[7] Yi Guo, Robert G. Parker, Stiffness matrix calculation of rolling element bearings using a finite element/contact mechanics model, Journal of Mechanism and Machine Theory (2012) 51: 32–45

[8] H Miao, C Zang and M I Friswell, Dynamic similarity design method for an aero-engine dual - rotor test rig, Journal of Physics: Conference Series 744 (2016) 012109

[9] R. Srinath, A. Sarkar, A. S. Sekhar, Parametrically Excited Vibration in Rolling Element Bearings, Inter. Noise conference, Melbourne, Australia (2015) 1 : 6

[10] Kovacic, I., Rand, R., and Mohamed Sah, S. "Mathieu's Equation and Its Generalizations: Overview of Stability Charts and Their Features." ASME. Appl. Mech. Rev. March 2018; 70(2): 020802. https://doi.org/10.1115/1.4039144

[11] Richard H. Rand, Lecture Notes on Nonlinear Vibrations, (2014), Cornell University

[12] D. Younesian, E. Esmailzadeh, R. Sedaghati, Asymptotic solutions and stability analysis for generalized non-homogeneous Mathieu equation, Journal of Communications in Nonlinear Science and Numerical Simulation, (2007) 12: 58 – 71

[13] Yusry O. El-Dib, Nonlinear Mathieu equation and coupled resonance mechanism, Journal of Chaos, Solitons and Fractals (2001) 12: 705 – 720

[14] C. S. HSU, On the Parametric Excitation of a Dynamic System Having Multiple Degrees of Freedom, Journal of Applied Mechanics (1963) 367 – 372

[15] W.Szemplińska-Stupnicka, The generalized harmonic balance method for determining the combination resonance in the parametric dynamic systems, Journal of Sound and Vibration (1978) 58(3): 347 – 361

[16] Qinkai Han Zhaoye Qin Jingshan Zhao Fulei Chu, Parametric instability of cylindrical thin shell with periodic rotating speeds, International Journal of Non – Linear Mechanics (2013) 54: 201 – 207

[17] Parametric instability of a Jeffcott rotor with rotationally asymmetric inertia and transverse crack, Journal of Nonlinear Dynamics (2013) 73: 827 – 842

[18] Parametrically instability of a rotor – bearing system with two breathing transverse cracks, European journal of mechanics (2012) 36: 180 – 190

[19] Torsional oscillations of a rotor with continuous stator contact, International Journal of Mechanical Sciences (2014) 83: 65 – 75

[20] Nonlinear dynamics of a Jeffcott rotor with torsional deformation and rotor – stator contact, International Journal of Non – Linear Mechanics (2017) 92: 102 – 110.

[21] Effects of high frequency drive speed modulation on rotor with continuous stator contact, International Journal of Non – Linear Mechanics (2017) 131 – 132: 559 – 571

[16] Ali H. Nayfeh, Balakumar Balachndran, Applied Nonlinear Dynamics, Computational, and Experimental Methods, JOHN WILEY & SONS, INC. (1995)

[17] A. H. Nayfeh, T. Mook, Nonlinear Oscillations, JOHN WILEY & SONS, INC. (1995)

[18] T. Bakri, R. Nabergoj, A. Tondl, F. Verhulst, Parametric excitation in non-linear dynamics, International Journal of Non-Linear Mechanics (2004) 39: 311 – 329

[19] Stefano Zucca and Bogdan I Epureanu, Reduced order models for nonlinear dynamic analysis of structures with intermittent contacts, Journal of Vibration and Control (2017) Volume: 24 issue: 12, page(s): 2591-2604

[20] Krack M., Gross J. (2019) Theory of Harmonic Balance. In: Harmonic Balance for Nonlinear Vibration Problems. Mathematical Engineering. Springer, Cham